Silica-scavenging effects in ceria-based solid electrolytes

D. IVANOVA, A. KOVALEVSKY, V.V. KHARTON, F.M.B. MARQUES

CICECO/Ceramics and Glass Eng. Dept.
University of Aveiro, 3810-193 Aveiro, Portugal

Composite materials based on gadolinium doped ceria (CGO) with additions of silica, with both silica and lanthanum oxide, and with lanthanum silicate, were prepared by the conventional ceramic route, to assess the silica scavenging role of lanthanum oxide additions. Structural, microstructural and electrical characterization of these samples confirmed the formation of one apatite type lanthanum silicate-based phase from reaction of silica with lanthanum oxide. The formation of this phase occurred in parallel with a significant enhancement of the grain boundary conductivity of these composite materials. Further interaction between constituents, involving diffusion of La to CGO, and Ce and Gd to the apatite phase, had no significant consequences on the electrical performance of these materials. Overall, lanthanum oxide was shown to remove the siliceous phases from the grain boundaries of CGO.

Keywords: ceria, scavenging effect, silica, grain boundary

Efecto de eliminación de sílice en electrolitos sólidos basados en óxido de cerio.

Se prepararon materiales compuestos basados en óxido de cerio dopado con gadolinio (TGO) con adicciones de sílice, con sílice y óxido de lantano y silicato del lantano, mediante procesamiento cerámico convencional con objeto de confirmar el papel secuestrante de sílice de las adicciones. La caracterización estructural, microestructural y eléctrica de las muestras confirmó la formación de una fase tipo apatito basada en silicato de lantano a partir de la reacción de la sílice con el óxido de lantano. La formación de esta fase ocurre en paralelo con un incremento significativo de la conductividad a través del borde de grano de estos materiales. La interacción entre los constituyentes, incluyendo la difusión del La al CGO, y el Ce y el Gd a la fase apatito, no tiene consecuencias significativas sobre el comportamiento eléctrico de estos materiales. Resumiendo, el óxido de lantano es capaz de eliminar las fases silicias del borde de grano del CGO.

Palabras clave: ceria, efecto secuestrante, sílice, borde de grano

1. INTRODUCTION

Fast ion conduction in solid electrolytes, a major requirement for current carrying devices like Solid Oxide Fuel Cells (SOFCs), is the combined result of large concentrations of ionic defects and high ionic mobility. Materials with the fluorite-type structure are amongst the most effective oxygen-ion conductors. The fluorite structure shows comparatively high oxygen-ion mobility and accepts high levels of anionic disorder, which can be introduced to compensate for aliovalent metal doping [1-2].

One of the most used fluorite-type oxides is yttria stabilized zirconia (YSZ). However, due to the relatively low ionic conductivity of zirconia-based electrolytes, the potential operating temperature range is reasonably high, requiring the use of expensive complementary materials. The conductivity of ceria-based oxides is larger than the electrical conductivity of YSZ. As an example, gadolinia doped ceria (CGO) at 800ºC has about the same conductivity of YSZ at about 1000ºC. For this reason, ceria-based ceramics received increasing attention during the last years [2-4].

The total conductivity of polycrystalline ceramics is a combination of the grain boundary and bulk grain contributions. The grain boundary conductivity is usually several orders of magnitude smaller than the bulk conductivity. Impurities in the grain boundary region partly explain this effect. In the low/intermediate temperature range, resistive grain boundaries are responsible for high ohmic losses preventing better electrolyte performance [5-8].

Silica is recognized to be the predominant constituent of the grain boundary region in many low grade ceramics, much cheaper than the high purity oxides adopted as state of the art electrolytes. The detrimental effect of silica in grain boundaries was firstly investigated in YSZ ceramics [5-6]. The addition of Al_2O_3 was found to reduce the grain boundary resistivity of YSZ ceramics due to removal of silica.

Bol. Soc. Esp. Ceram. V., 47, 4, 201-206 (2008)

201

A possible explanation for this so-called scavenging effect is that silica combines with Al_2O_3, namely due to preferential wetting of this phase, becoming localized in small regions, frequently in triple contact points between YSZ grains. Al_2O_3 is recognized to be the most effective additive to promote the silica scavenging effect in YSZ. Segregation of SiO_2 impurities along the grain boundaries causes a deleterious effect on the total conductivity of CGO ceramics [7-8]. However, alumina additions to CGO ceramics showed a deleterious effect due to formation of another non-conductive phase, $GdAlO_3$ [7].

The conductivity of materials derived from the nominal $La_{10}(SiO_4)_6O_3$ apatite-type phase is close to that of CGO, especially in the intermediate temperature range [9-11]. The high oxygen conduction of apatites justified the attempt to form this phase in low-grade YSZ powders from reaction of La_2O_3 with silica. Previous work proved that this addition of La_2O_3 was indeed effective. However, simultaneous formation of lanthanum zirconate, a well known poorly conducting reaction product from zirconia and lanthanum oxide, prevented better overall results [12]. The present work was conducted to evaluate the improvement of the oxygen ion transport properties of silica-containing CGO based electrolytes. The rationale for this approach was that the interaction between this electrolyte and lanthanum oxide should be considerably different from the above mentioned role in the presence of zirconia.

2. EXPERIMENTAL PROCEDURE

Commercially available $Ce_{0.8}Gd_{0.2}O_{2-\delta}$ (Rhodia), SiO_2 (Merck) and La_2O_3 (Aldrich) high purity powders were used as starting materials. All compositions (including $Ce_{0.8}Gd_{0.2}O_{2-\delta}$ - CGO, CGO with silica addition - CGOSi, CGO with addition of lanthanum silicate - CGOLS, and CGO with addition of silica and lanthanum oxide - CGOLS-ox were prepared using the conventional ceramic processing route. In the latter case, lanthanum oxide was added in adequate proportions to fully combine with silica as $La_{9.33}Si_6O_{26}$ - LS, forming this conductive apatite phase as part of the scavenging effect.

Pure CGO and compositions containing different amounts of silica were used as reference. The lower additions of silica (0.5 mol %) were chosen taking into account typical levels of silica impurities in low-grade CGO powders (Si > 100 ppm). However, sometimes such small quantities (or derived phases) are difficult to identify by XRD and/or SEM/EDS. To provide a better basis for analyses an additional set of compositions was investigated where the amount of additives was 5 mol % (with reference to the SiO_2 addition).

The apatite (LS) as additive was synthesized at 1200°C during 6h, starting from SiO_2 and La_2O_3 oxides, before mixing and joint sintering with CGO.

Stoichiometric amounts of all powders were mixed with ethanol in a ball mill for 2-4 h, with zirconia milling media. The slurries of all compositions were dried and the obtained powders homogenized and mixed (agate mortar) with polyvinyl alcohol (PVA) as binder. This improved the powders ability for shaping. Afterwards, powders were uniaxially pressed (220 MPa) into cylindrical pellets. A variety of temperature/time conditions was exploited for the fabrication of dense ceramics, starting from a plateau at 1500°C for 4 h to a plateau at 1650°C for 4 h. Sintering was performed in air with a constant heating rate of 5°C/min and cooling rate of 3°C/min.

Values and final densities of pellets were calculated from the mass and geometrical dimensions of the pellets. The samples were analyzed by X-ray diffraction. The XRD patterns were collected at room temperature (CuK_α, $2\theta=20-70°$, step 0.02°, 1 s/step).

The bulk and grain boundary resistances of sintered pellets were obtained by ac impedance spectroscopy in air using one HP Impedance Analyzer (HP4284A precision LCR meter). Symmetrical platinum electrodes were applied on both surfaces of the pellet using Pt paste fired at 1000°C during 2h. The electrical measurements were performed from 200°C to 1000°C, in the range of 20–10^6 Hz, with an excitation voltage of 500 mV. In order to obtain a high resolution of impedance arcs, samples with low length to electrode surface area (L/S) were used (L/S ~ 0.35 cm^{-1}).

3. RESULTS AND DISCUSSION

3.1 Structural and microstructural characterization

Several attempts were made to identify effective sintering conditions for the ceria-based ceramics. The sintering, pressing and milling conditions listed in Table 1 describe briefly the range of preparation parameters and corresponding results. It was found that the highest relative density of materials was achieved after sintering during 4 h at 1650°C pellets previously pressed at 220 MPa. This set of conditions was adopted for all samples studied in this work. Reaching such a high sintering temperature was not within the goals of the present work due to the risk of degradation of electrical performance by inter-diffusion of constituent cations. Nevertheless, the experimental conditions used are only meaningful if able to provide pellets with densifications in excess of about 92%

TABLE 1. SINTERING CONDITIONS AND DENSITY OF THE SAMPLES.

Attempt	Sintering T, °C	Sintering time, h	Pressure, MPa	Ball-milling, h	Composition	Relative density, %
1	1600	2	20	2	CGO	84.9
					CGOLS-0.5%	78.6
2	1500	4	180	2	CGO	86.3
					CGOLS-0.5%	76.9
3	1550	4	180	2	CGO	86.6
					CGOLS-0.5%	81.6
4	1600	4	180	4	CGO	89.7
					CGOLS-0.5%	87.8
5	1650	4	220	4	CGO	93.7
					CGOLS-0.5%	93.2

of the theoretical density to avoid open porosity. Lower densifications are hardly acceptable in electrolyte layers for technological devices like SOFCs.

The XRD patterns of the CGO and silica-containing ceramics were refined using the WinPLOTR and FullProf suite to identify the corresponding phases and to obtain the lattice parameters of phases shown in Table 2. At high sintering temperatures such as 1650°C, the formation of gadolinium silicate grains was detected by XRD in CGOSi compositions, as shown in Fig.1 and Table 2. The decrease of the lattice parameters of CGO in silica-containing samples can be explained by loss of gadolinium to the silica-based secondary phase, due to lixiviation from CGO and formation of the gadolinium-containing apatite. The lattice parameters of the apatite phase (clearly present namely in CGOSi-5% specimens) are larger than found for pure $Gd_{9.33}(SiO_4)_6O_2$. This is probably due to the formation of one $Gd_{9.33}(SiO_4)_6O_2$-based solid solution containing a small amount of cerium. The formation of the metastable $Ce_{9.33}(SiO_4)_6O_2$ phase is less likely.
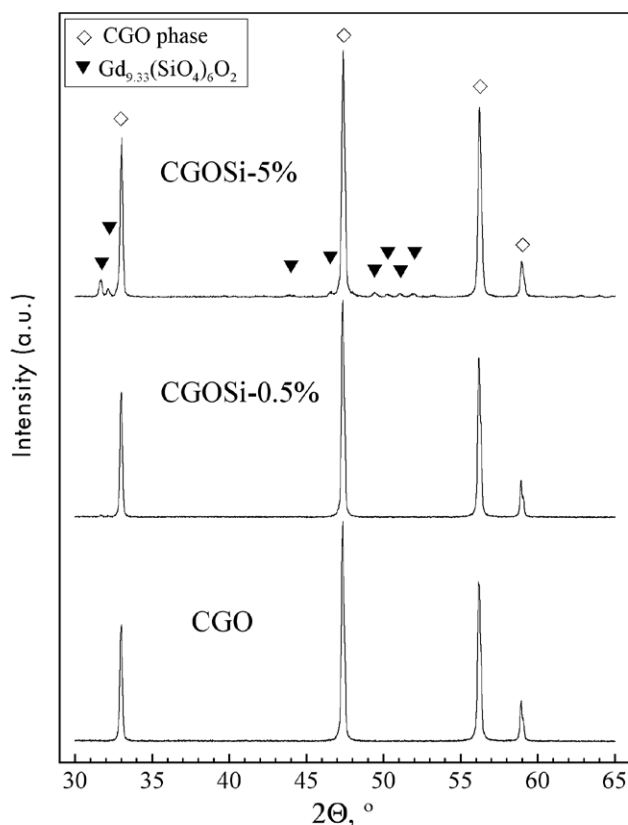

(a)

(b)

(c)

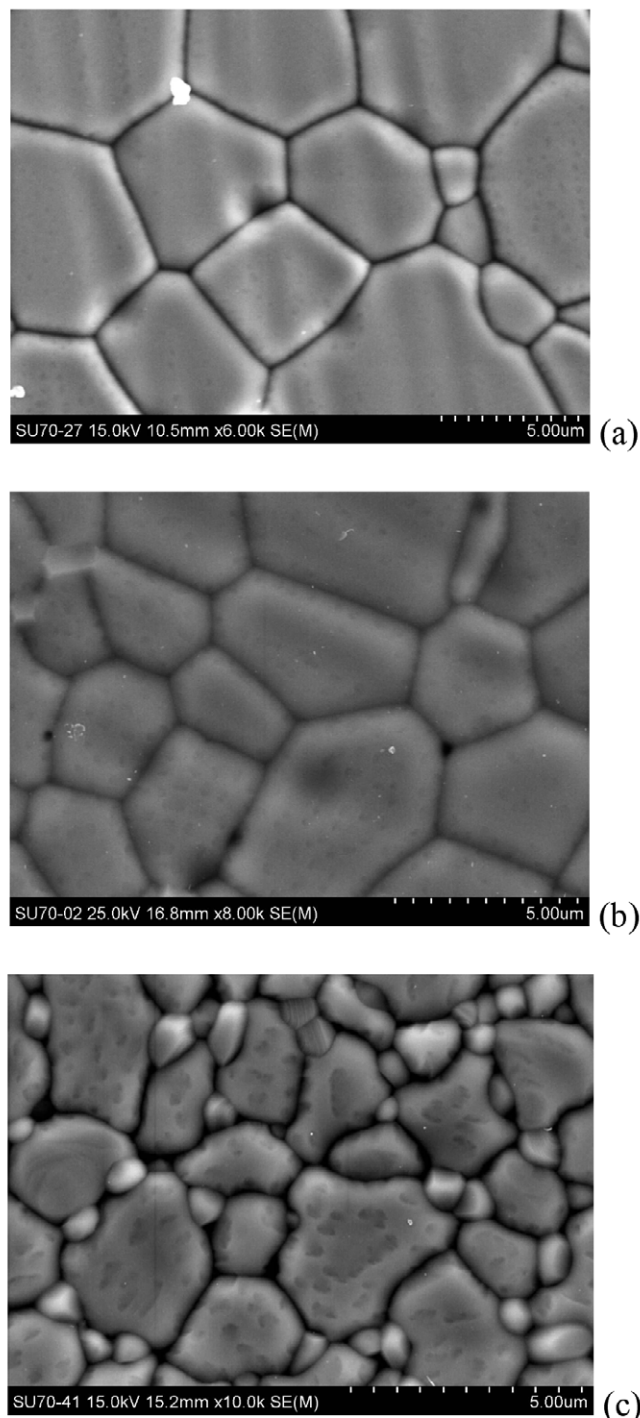Fig. 1- XRD patterns of sintered CGO and CGOSi (0.5 and 5%) samples.

Fig. 2- Microstructure of the CGO (a), CGOSi-0.5% (b) and CGOSi-5% (c) samples.

TABLE 2. LATTICE PARAMETERS OF CGO-BASED PHASES AND APATITES IN SEVERAL SAMPLES

Lattice parameter of CGO-based phases		Lattice parameters of apatite phases		
Nominal composition	Parameter a, Å	Composition	Parameter a, Å	Parameter c, Å
pure CGO	5.4328	$Gd_{9.33}(SiO_4)_6O_2$ [13]	9.431	6.873
		$La_{9.33}(SiO_4)_6O_2$ [13]	9.713	7.194
CGOSi-0.5%	5.4265	mixed apatite	9.4690	6.8739
CGOSi-5%	5.4216	mixed apatite	9.4635	6.8770
CGOLS-0.5%	5.4270	mixed apatite	9.5901	7.0030
CGOLS-5%	5.4379	mixed apatite	9.5978	7.0106

Bol. Soc. Esp. Ceram. V., 47, 4, 201-206 (2008)
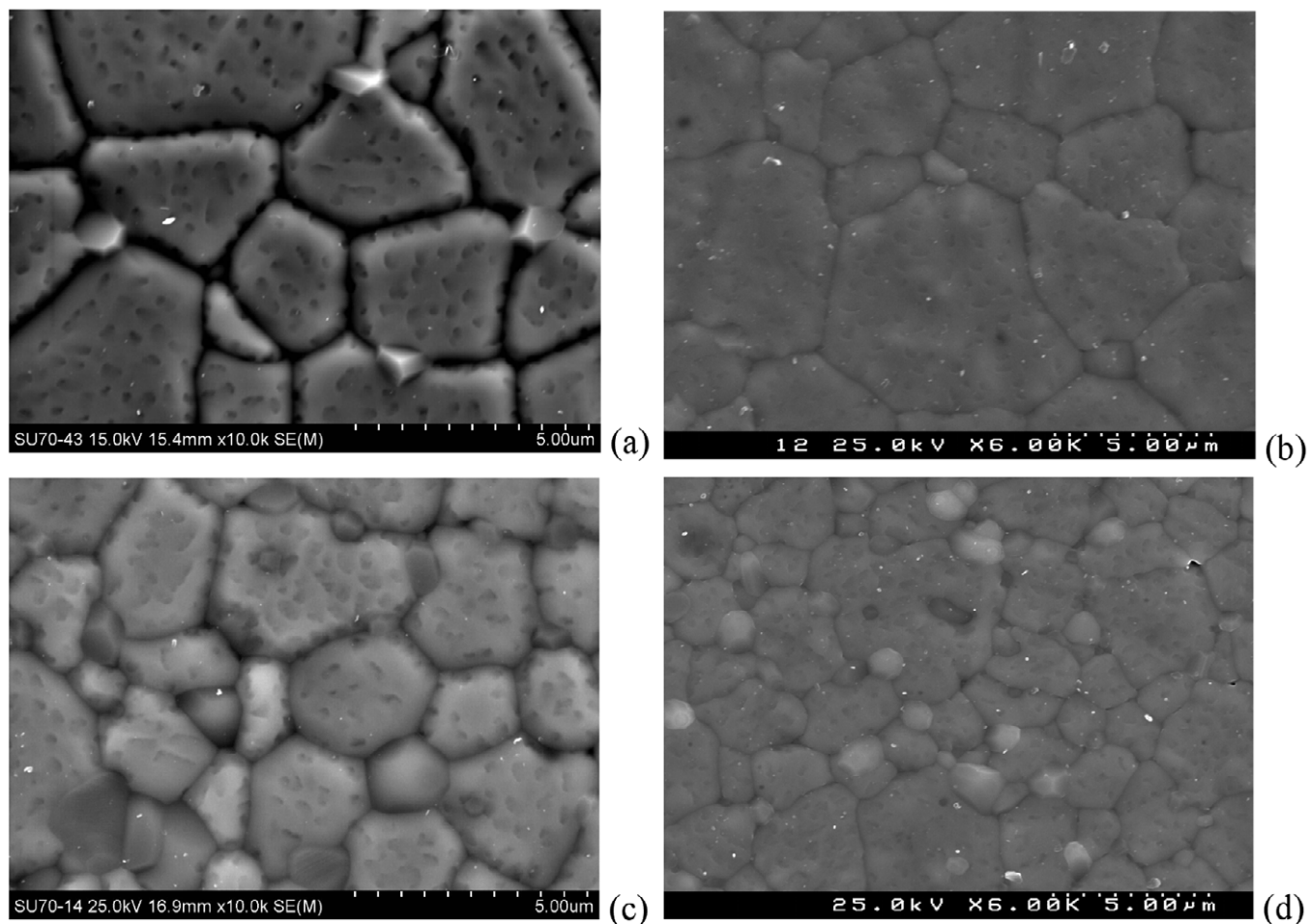
203

Fig. 3- SEM micrographs of the CGOLS-0.5% (a), CGOLS-ox-0.5% (b), CGOLS-5% (c) and CGOLS-ox-5% (d) samples.

While the lattice parameters of CGO increased in CGOLS-5% with respect to pure CGO, there is a slight decrease in the lattice parameters of the apatite phase (LS). This observation also indicates that some La^{3+} dissolved in the ceria lattice, as the ionic radius of La^{3+} is higher than that of Ce^{4+}. This fact is not surprising considering the solubility of La_2O_3 in ceria, recently confirmed [14]. However, XRD analysis showed no evidence for the presence of free silica in the CGOLS-5% sample, probably, due to co-existence of various types of apatites in CGOLS, or for being below the detection limit (Table 2).

Examples of microstructures of selected materials are shown in Figs. 2 and 3. In the first case, the role of single silica additions is emphasized. For low silica additions, the CGO-based electrolyte shows a rather homogeneous microstructure, without any clear evidence of the presence of a second phase. Due to the low amount of silica present in this material, this phase could be easily spread along the grain boundaries, either free or combined with gadolinium, as suggested from the XRD data. A similar observation was previously reported for identical additions of silica to YSZ [12]. For samples with high amounts of silica, a second phase is clearly present, dispersed between the CGO-based grains. The formation of this new phase, from interaction between silica and gadolinium oxide, was confirmed by combined SEM/EDS analysis.

Fig. 3 shows the microstructures of samples with lanthanum silicate, either directly added to CGO or formed during high temperature sintering with silica and lanthanum oxide. The presence of a second phase is also obvious in this case, with small grains dispersed throughout the dominant CGO-based phase.

Summarizing, the microstructural characterization of all these samples showed two major groups of materials. In the first group (pure CGO and CGO with low silica content) the material seemed homogeneous, with regular grain size and no visible presence of any secondary phase. In the second group of materials (CGO with large amounts of silica and all samples with LS), the microstructure was typical of a composite, with the secondary phases spread throughout the CGO-based matrix, apparently as isolated grains located in the grain boundaries of the dominant phase. These comments are needed to discuss the electrical performance of these materials in the next section.

3.2 Impedance spectroscopy

To confirm the scavenging effect of La_2O_3 additions with respect to silica as impurity, the conductivities of pure CGO, silica-containing CGO and apatite-containing CGO were investigated. The transport properties of selected samples were analysed by impedance spectroscopy in air. This provided estimates for the total resistivity of the material and, at the same time, information on the so-called bulk and grain boundary contributions. As siliceous phases tend to spread
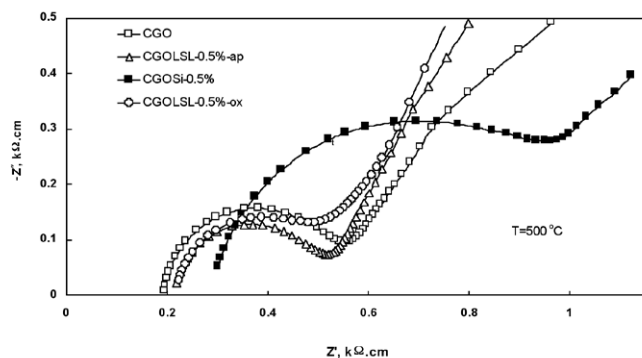
Fig. 4- Impedance spectra obtained at 500°C in air for CGO, CGOSi-0.5% and apatite-containing samples.

along the grain boundaries, the presence and/or removal of these phases should be easily noticed with this type of measurements.

The impedance spectra of CGO, silica-containing samples and apatite containing samples, at 500°C, are shown in Fig. 4. The branches of the low frequency response are due to electrode effects, while the high and intermediate frequency arcs describe the bulk and grain boundary performance of these compositions. At this temperature (500°C), it is impossible to see the arcs attributed to the bulk grain contribution due to the limited frequency range of the equipment. However, due to the good definition of the intermediate frequency arcs (typically within the range 5 kHz to 1 MHz at 500°C), the values of bulk resistivity of these samples were easily calculated from the visible parts of the impedance spectra, namely from estimates of the high frequency intercepts of the grain boundary arcs.

Fig. 4 shows that the bulk resistivity of the silica-containing sample is higher than all the others. Pure CGO and the apatite containing samples show almost the same bulk resistivity. The decrease in the bulk grain conductivity of the silica-containing ceramics is probably due to loss of gadolinium from CGO grains, as a consequence of the formation of a gadolinium-based apatite. This fact agrees quite well with the previous discussion on phase identification and lattice parameters of CGO-based phases (Table 2).

The total conductivity of all these materials is mainly governed by the grain boundary contribution at this and lower temperatures. As can be seen in Fig. 4, the so-called "macroscopic" grain boundary resistivity of CGO ceramics is greatly influenced by the simple addition of silica to CGO ceramics. Here the term "macroscopic" is used to enhance the fact that these values were estimated using the macroscopic shape of the sample (length and area). Since gadolinium silicate is a poorly conducting phase, the presence of $Gd_{9.33}(SiO_4)_6O_2$ layers along the grain boundaries of CGO ceramics would increase the grain boundary resistivity of the base material. The possible presence of siliceous thin layers along the grain boundaries of the CGO grains would also contribute in a similar manner to the observed large grain boundary impedance in silica containing CGO ceramics. Both effects might explain the enhancement of the grain boundary impedance by a factor of two or three in the case of light silica addition.

Another type of behaviour is observed for the CGOLS and CGOLS-ox samples, where the apatite phase was introduced in different manners (from pre-synthesized apatite and from

joint reaction/sintering directly from the constituent oxides). As shown in Fig. 4, the grain boundary conductivity was greatly improved by the formation of the $La_{9.33}(SiO_4)_6O_2$-based solid solution in the CGOLS-ox sample. The removal of siliceous layers from the grain boundaries of CGO together with the formation of the apatite conductive phase improves the grain boundary conductivity of this material with respect to the simple presence of silica.
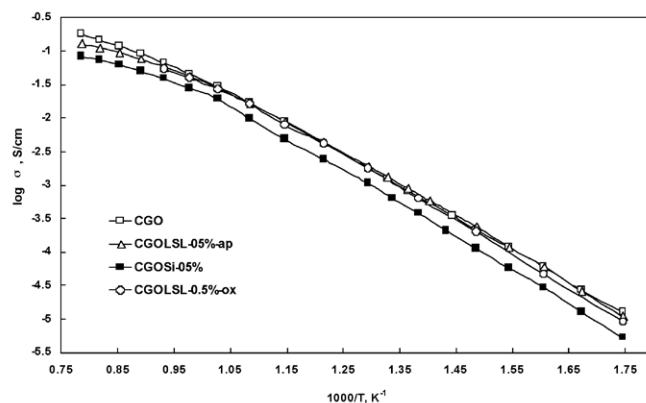

Fig. 5- Arrhenius plot of total conductivity in air of CGO, CGOSi-0.5% and CGOLSL-0.5% samples.
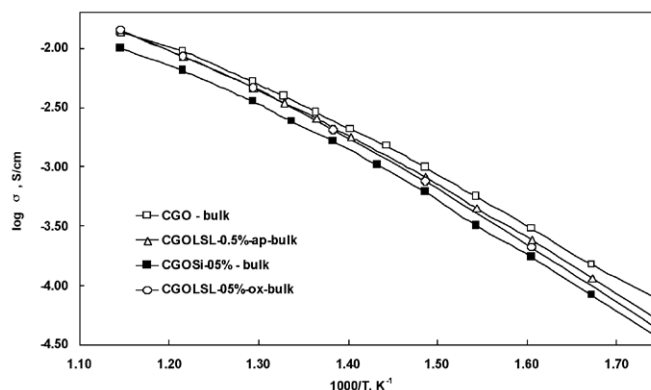

Fig. 6- Arrhenius plot of bulk contribution to total conductivity of CGO, CGOSi-0.5% and CGOLSL-0.5% samples.
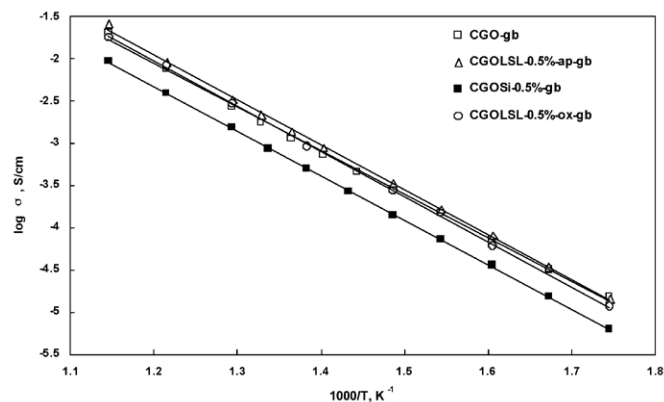

Fig. 7- Arrhenius plot of grain boundary contribution to the total conductivity of CGO, CGOSi-0.5% and CGOLSL-0.5% samples.

The impedance spectra obtained at several temperatures were fitted assuming a series association of R-(RQ) terms (where R is a resistance and Q a pseudo-capacitance/constant

phase element), taking into account that arcs were slightly depressed. The fitting parameters were used to estimate the grain boundary, bulk and total conductivity of the samples by simple conversion of the resistance to electrical conductivity, taking into consideration the sample geometry, as already mentioned. The total conductivity of all samples is shown in Fig. 5 using one typical Arrhenius representation. It can be seen from this Arrhenius plot that the total conductivity of the silica-containing sample is significantly lower, while the total conductivities of pure CGO and apatite-containing samples are almost coincident. In order to see the actual grain boundary and bulk behaviour, conductivities attributed to the grain interior and grain boundary are also plotted in Figs. 6 and 7. As mentioned before, the silica-containing CGO ceramics show always the worst transport properties. The activation energies are in all cases close to each other, as expected for the type of phenomena involved.

A final remark should be introduced on the interesting performance of CGO+LS composites. XRD and combined SEM/EDS analysis showed clearly a strong interaction between phases, with La diffusion to CGO and loss of Gd to the silicate phase. This observation together with a good electrical performance of these samples is coherent with the reported optimized transport properties of fluorite based electrolytes containing more than one dopant [15-17].

4. CONCLUSIONS

The formation of CGO-based composites from reaction between oxides was exploited to improve the electrical properties of ceria based ceramics with silica as impurity. The formation of apatites as minor secondary phases provided the predicted silica scavenging effect. The formation of the apatite phase improved to a great extent the grain boundary conductivity of these silica-containing materials, without loss of bulk conductivity. The formation of other possible compounds from reaction between lanthanum oxide and CGO was not detected, although inter-diffusion was found to occur to a reasonable extent. The interesting performance of these materials suggests some room for the search of improved electrolytes based on ceria with more than one dopant cation.

ACKNOWLEDGEMENT

◆ ◆ ◆

REFERENCES

1. B.C.H. Steele, B.E. Powell and P.M.R. Moody, Anionic Conduction in Refractory Oxide Solid Solutions Possessing the Fluorite, Pyrochlore and Perovskite Structures, Proc. Brit. Ceram. Soc., 10 (1968) 87-102.
2. V.V. Kharton, F.M.B. Marques, A. Atkinson, Transport properties of solid oxide electrolyte ceramics: a brief review, Solid State Ionics, 174 (2004) 135– 149.
3. H. Inaba, H. Tagawa, Ceria-based solid electrolytes, Solid State Ionics, 83 (1996) 1- 16.
4. B.C.H. Steele, Appraisal of $Ce_{1-y}Gd_yO_{2-y/2}$ electrolytes for IT-SOFCs operation at 500°C. Solid State Ionics, 129 (2000) 95–110.
5. E. P. Butler and J. Drennan, Microstructural Analysis of Sintered High-Conductivity Zirconia with Al2O3 Additions, J. Am. Ceram. Soc., 65 [10] (1982) 474-478.
6. X. Guo, Chao-Qun Tang, Run-Zhang Yuan, Grain Boundary Ionic Conduction in Zirconia-based Solid Electrolyte with Alumina Addition, J. Eur. Ceram. Soc., 15 (1995) 25-32.
7. T. Zhang, Z. Zeng, H. Huang, P. Hing, J. Kilner, Effect of alumina addition on the electrical and mechanical properties of $Ce_{0.8}Gd_{0.2}O_{2-\delta}$ ceramics, Materials Letters 57 (2002) 124–129.
8. T.S. Zhang, J. Ma, L.B. Kong, S.H. Chan, P. Hing, J.A. Kilner, Iron oxide as an effective sintering aid and a grain boundary scavenger for ceria-based electrolytes, Solid State Ionics 167 (2004) 203–207.
9. S. Nakayama, T. Kageyama, H. Aono and Y. Sadaoka, Ionic Conductivity of Lanthanoid Silicates, $Ln_{10}(SiO_4)_6O_3$ (Ln = La, Nd, Sm, Gd, Dy, Y, Ho, Er and Yb), J. Mater. Chem., 5 (1995) 1801-1805.
10. S. Tao, J.T.S. Irvine, Preparation and characterization of apatyte-type lanthanum silicates by a sol-gel process, Mat. Res. Bull., 36 (2001) 1245-1258.
11. A.L. Shaula, V.V. Kharton, F.M.B. Marques, Oxygen ionic and electronic transport in apatite-type $La_{10-x}(Si,Al)_6O_{26-\delta}$, J. Sol. St. Chem., 178 (2005) 2050–2061.
12. A. V. Kovalevsky, F. M. B. Marques, V. V. Kharton , F. Maxim, J. R. Frade, Silica-scavenging effect in zirconia electrolytes: assessment of lanthanum silicate formation, Ionics 12 (2006) 179–184.
13. L. Li, D.M. Strachan, H. Li, L.L. Davis, M. Qian, Crystallization of gadolinium- and lanthanum_containing phases from sodium alumino-borosilicate glasses, J. Non-Crystalline Sol., 272 (2000) 46-56.
14. M. Hrovat, J. Holc, S. Bernik, and D. Makovec, Subsolidus phase equilibria in the $NiO-CeO_2$ and $La_2O_3-CeO_2-Fe_2O_3$ systems, Mat. Res. Bull., 33, 8 (1998) 1175–1183.
15. S.K. Tadokoro, E.N.S. Muccill, Effect of Y and Dy co-doping on electrical conductivity of ceria ceramics, J. Eur. Ceram. Soc., 27 (2007) 4261-4264.
16. X. Sha, Z. Lü, X. Huang, J. Miao, Z. Ding, X. Xin and W. Su, Study on La and Y co-doped ceria-based electrolyte material, J. Alloys and Compounds 428 (2007) 59-64.
17. S. Omar, E.D. Wachsman, J.C. Nino, A co-doping approach towards enhanced ionic conductivity in fluorite-based electrolytes, Solid State Ionics 177 (2006) 3199-3203.